15-2-2006

The Cape Grim Scanning UV Spectrometer

Stephen R. Wilson
University of Wollongong, swilson@uow.edu.au

The Cape Grim Scanning UV Spectrometer

Abstract

The scanning spectral radiometer operating at Cape Grim provides estimates of irradiance for several spectral regions between 298 and 400 nm. The physical characteristics of the spectrometer system are documented, including the wavelength shift and cosine response of the detector head. The procedures used for the spectrometer's in situ calibration are also described. The scatter in the resulting calibrations is quantified for the period between 2000 and 2003, providing an estimate of the (wavelength dependent) uncertainty in the measurement.

Keywords

UV Spectrometer, measurement, calibration, GeoQUEST

Disciplines

Life Sciences | Physical Sciences and Mathematics | Social and Behavioral Sciences

Publication Details

This article was originally published as Wilson SR, The Cape Grim Scanning UV Spectrometer, in Cainey, JM, Derek, N and Krummel, PB (eds), Baseline Atmospheric Program (Australia) 2003-2004, Australian Bureau of Meteorology and CSIRO Marine and Atmospheric Research, February 2006, 9-16.

Baseline 2003 - 2004

THE CAPE GRIM SCANNING UV SPECTROMETER

S R Wilson

Edited by J. M. Cainey, N. Derek and P. B. Krummel
Australian Bureau of Meteorology and CSIRO Marine and Atmospheric Research, Melbourne

Published for the Australian Bureau of Meteorology and
CSIRO Marine and Atmospheric Research, Melbourne

ISBN 1 921061 33 2

THE CAPE GRIM SCANNING UV SPECTROMETER

S R Wilson

Atmospheric Chemistry Research Group, Department of Chemistry,
University of Wollongong, Wollongong, NSW 2522, Australia

Abstract

The scanning spectral radiometer operating at Cape Grim provides estimates of irradiance for several spectral regions between 298 and 400 nm. The physical characteristics of the spectrometer system are documented, including the wavelength shift and cosine response of the detector head. The procedures used for the spectrometer's *in situ* calibration are also described. The scatter in the resulting calibrations is quantified for the period between 2000 and 2003, providing an estimate of the (wavelength dependent) uncertainty in the measurement.

1. Introduction

The significant global changes in stratospheric ozone observed in the last ~3 decades have been intensively studied [Chipperfield *et al*., 2003], and this has been paralleled by an effort to detect the resulting changes in the amount of solar UV-B reaching the earth [Kerr *et al*., 2003; McKenzie *et al*., 2003]. While UV trends have been observed [McKenzie *et al*., 2003], the solar radiation reaching the earth's surface, and especially the UV-B (280 - 315 nm), is also strongly affected by a range of other factors, including cloudiness and aerosol scattering, so that climatological changes can readily mask any ozone driven trends.

The UV-B region has a wide range of impacts, including on health [de Gruijl *et al*., 2003], biota [Caldwell *et al*., 2003; Hader *et al*., 2003; Zepp *et al*., 2003] and manmade structures [Andrady *et al*., 2003]. The UV-B and UV-A regions are also critical for several key photochemical reactions. One pivotal process is the photolysis of ozone to produce O (^{1}D),

$$O_3 + h\nu \xrightarrow{J(O(^1D))} O + O(^1D)$$

which is driven by wavelengths around 310 nm. In the clean atmosphere this process is the dominant factor in determining the OH concentration [Creasey *et al*., 2003], which in turn is the main atmospheric oxidant.

Another important photochemical reaction involves NO_2:

$$NO_2 + h\nu \xrightarrow{J(NO_2)} NO + O$$

The reaction is driven by wavelengths between 300 and 410 nm in the troposphere. The intensity of radiation in this region therefore determines the balance between NO and NO_2 [Atkinson *et al*., 2004; Sander *et al*., 2002], which then alters the fate of many other organic compounds in the atmosphere.

For these reasons it is important to have a record of UV radiation at sites like Cape Grim where the interference from nearby human activity is minimised. Various UV measurements have been made at Cape Grim, including the long-term deployment of a broadband UV-A monitor in the early 1980s. A measurement program involving a scanning UV spectrometer was initiated in 1992, with a system developed that permits automatic operation. The system is designed to measure global and diffuse irradiance alternately in the UV-B and UV-A region. In this paper the system currently in operation will be outlined, including the operational configuration, the calibration procedure and the system performance.

2. Experimental description

The spectral radiometer system (known as SRAD), is shown schematically in Figure 1. SRAD consists of a spectrometer, a sun-tracker and instrument controller. The individual components in current use will now be outlined.

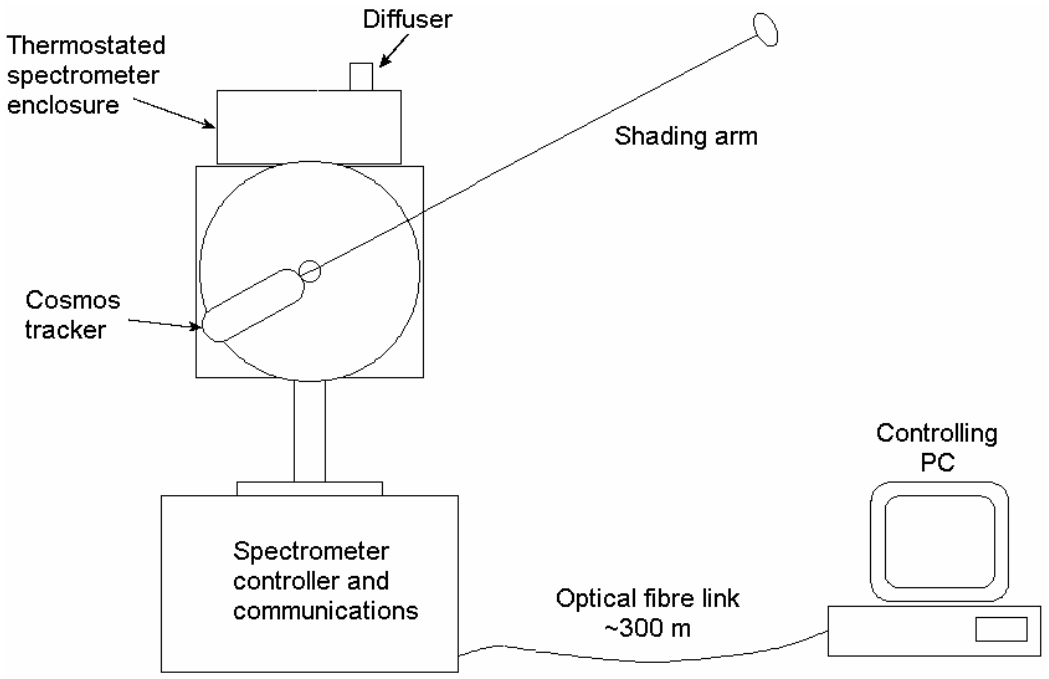

Figure 1. A schematic of the instrumental layout for SRAD. The instrument is located in the radiation enclosure, with the controlling computer housed within the Cape Grim laboratory.

2.1. Optical system

The input optic is a PTFE diffuser with a raised dome and rim, purchased from NIWA, NZ (http://www.niwascience.co.nz/rc/instruments/lauder/ptfe) (Bo-5.3) with deviations from ideal (cosine) response of less than 3% for angles less than 75°. For isotropic radiation the correction for non-ideality for this diffuser is of the order of 1%. A recent survey [Pye and Martin, 2000] found that diffusers of this general design have been found to have the smallest geometric errors. The diffuser used in SRAD has a directional response error (f_2) of 2.2%, significantly less than that observed for most diffusers reviewed [Pye and Martin, 2000].

The diffuser is coupled to the monochromator using a UV enhanced liquid light guide (Lumatec model 300). The spectrometer is an Optronics Model OL752, a compact double-monochromator, configured with 0.125 mm/0.5 mm/0.125 mm width slits to give a nominal resolution of 1 nm (Full Width at Half Maximum, FWHM). The spectrometer has been modified by removal of the internal UG-11 ultraviolet filter which degraded rapidly and led to poor instrumental line shape and instrument sensitivity. Also, the height of the middle slit was reduced by one third. The optical configuration of the spectrometer causes significant optical aberration, as evidenced by the distorted image observed on the central slit. The reduction of the height of the middle slit significantly improved the instrumental line shape (removing most of the line shape asymmetry, while still giving reasonable total light throughput). The final line shape of the instrument is close to Gaussian, as shown in Figure 2.

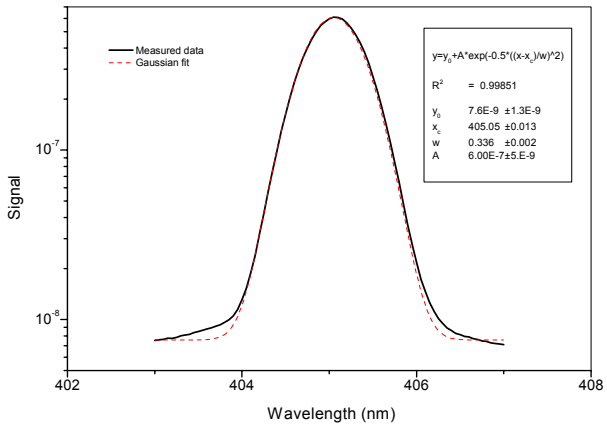

Figure 2. Plot of the observed SRAD signal looking at an atomic emission line from a low pressure mercury lamp. The fit is shown for a simple Gaussian. The instrumental line width is measured to be 0.8 nm, Full Width at Half Maximum.

The digitisation of the photomultiplier signal is 'adaptive', which means that a longer time is taken to integrate smaller (noisier) signals than larger signals. In practice this means that the time taken to collect a spectrum is variable, with longer times required under low light conditions (e.g. cloud, short wavelengths). For this reason it is necessary to record the time of the measurement at each wavelength, rather than the time at the start and end of the spectral scan.

The spectrometer is located in a housing which has the diffuser mounted on the upper lid. This housing is mounted on the top of the Cosmos Mk IV (Sci-Tec instruments) azimuth/elevation tracker, which has a shading arm affixed to the elevation drive. The spectrometer is temperature controlled to approximately 27°C using a 200 W resistive heater. This is essential as the spectrometer is quite tem-

perature sensitive, both in wavelength (0.07 nm/°C) and sensitivity (up to 6%/°C at 368 nm). With the temperature controller in operation, the calculated wavelength shifts (see later) have a standard deviation of around 0.013 nm, determined by both spectral noise and any spectrometer temperature change. This is consistent with a spectrometer temperature control of around ±0.1°C. This temperature control does not control the temperature of the diffuser.

2.2. *Sun tracker*

A crucial component of this system is the sun-tracking system. The position of the tracker required to shade the diffuser is calculated from the time of day and knowledge of the geometry of the system. The Cosmos tracker has a friction drive system for both axes. Under conditions of load, generated particularly by windy conditions, both axes can slip out of registration. For this reason, the tracker is returned every hour to a zero position, which is determined by mechanical stops within the tracker.

With the current configuration, for the central dome of the diffuser to remain totally shaded, and hence give a reliable estimate of the diffuse irradiance, the errors from the tracker need to be less than 0.3°. A plot of the cumulative fraction of the tracker errors for the calendar years between 2000 and 2003 is shown in Figure 3. At the end of 1999 the drive systems of both axes were overhauled, and the elevation drive rotated so that an unworn part of the friction drive disk was being used. In 2000, over 93% of all zero errors were less than 0.25°.

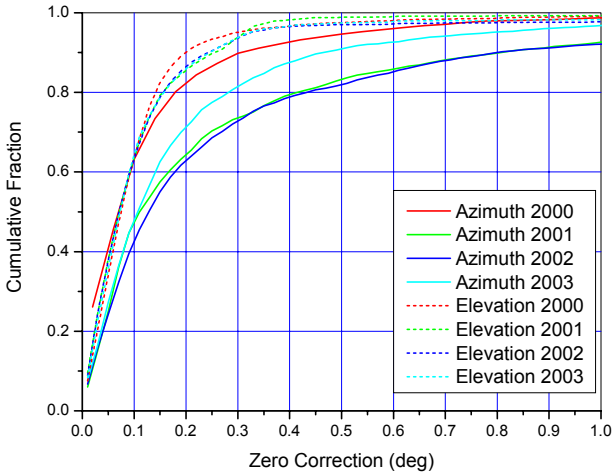

Figure 3. Cumulative fraction of tracker errors for the calendar years 2000 – 2003.

The azimuth drive slowly deteriorated through the period, although a major cleaning of the drive in 2002 did lead to an increase in reliability. The performance of the azimuth drive is worse before noon, as the drive must travel further from the zero (reference) point. For example, in 2002, 62% of the mornings met the 0.25° requirement, whereas 80% met the afternoon requirement. It is difficult to detect the impact of this by looking at clear sun measurements. However, at Cape Grim it is very rare for the early mornings to be unaffected by cloud.

2.3. *Instrumental control*

The tracker/spectrometer system is located in the radiation enclosure at Cape Grim (see site plan p 2), with communication to main laboratory via an optical fibre. The spectrometer and tracker are controlled by a PC using two RS232 serial communication ports. Software on the PC (written in Visual Basic) controls the instruments, collects the data (time of each measurement, wavelength, detector signal, and tracker status) and copies the resultant data files to the file server.

The wavelength region scanned by the instrument is a balance between several factors: (i) a desire to cover as large a wavelength region as possible; (ii) the need to make measurements at wavelength increments that permit reliable interpolation for the correction of the wavelength scale; (iii) the requirement that measurement be made at the wavelength of the sunphotometer (for calibration); and (iv) the need to measure frequently enough to permit reliable interpolation between spectral scans. The wavelengths scanned are summarised in Table 1, and are divided into three regions. Region 1 spans the majority of the UV-B and the higher end of the UV-A. The short wavelength limit has been determined by the requirements of calibration. The calibration methods outlined below give results which diverge below 300 nm due to the low signal. Region 2 is chosen to match with the sunphotometer wavelength and region 3 covers the end of the UV-A region and contains spectral features that can be used for wavelength calibration. A full scan typically takes 330 seconds.

Table 1. Wavelength scanning table for SRAD.

Region	Wavelength Start (nm)	Wavelength End (nm)	Wavelength Step (nm)
1	298.0	334.9	0.30
2	338.0	345.2	0.40
3	390.0	400.0	0.25

3. Calibration overview/outline

As outlined above, SRAD returns signal values (current) for each wavelength measured (S_λ), where the spectra are either of global or diffuse irradiance. To be useful the spectrometer signals need to be converted into irradiance (W m^{-2} or W m^{-2} nm^{-1}), which is the process of calibration. The calibration is a multi-step process, much of which is documented elsewhere [Wilson and Forgan, 1995]. Only an overview will be presented here, highlighting modifications to the published methodology.

3.1. *Wavelength scale calibration*

The wavelength of each measurement is determined by the mechanical positioning of the two spectrome-

ter gratings, a process that depends intimately upon the quality and condition of the optical and mechanical components. These change with time, due to both wear and temperature. As a result the wavelength scale of the instrument changes with time. The wavelength scale is checked using 5 mercury lines between 298 and 405 nm, measured from a low pressure mercury lamp, approximately twice a year. The recorded spectra allow assessment of the instrumental line shape (see Figure 1) as well as the absolute wavelength scale.

However, the wavelength scale needs to be determined for every scan. This is carried out by comparing the spectra with a reference spectrum in two wavelength regions (323.8-334 nm and 390-400 nm) using the method of Slaper *et al.* [1995]. The regions have been chosen so that they are not significantly affected by ozone absorption and have sufficient structure to allow a good correlation between the reference and recorded spectrum to be determined. As a reference spectrum, the extraterrestrial reference spectrum from the ATLAS 3 Solar Ultraviolet Spectral Irradiance Monitor (SUSIM) [M. E. van Hoosier, personal communication, 1996] has been used. The SUSIM spectrum has been convolved with a Gaussian approximation to the line shape of the instrument. A linear correction function is calculated using these two regions which is then applied to the data. As an example, the shift data derived for 2003 are shown in Figure 4. It can be seen that the correction of wavelength 'span' is small (representing a mean change in wavelength calibration of 0.1 nm over 100 nm) and stable (standard deviation of around 0.06 nm/100 nm) for the year, but that the absolute value of the correction shows significant step changes, occurring when the spectrometer is turned off. The two manual calibrations using a mercury lamp are included on the graph, and it can be seen that the results obtained by the lamp are indistinguishable from the value determined from the solar spectra.

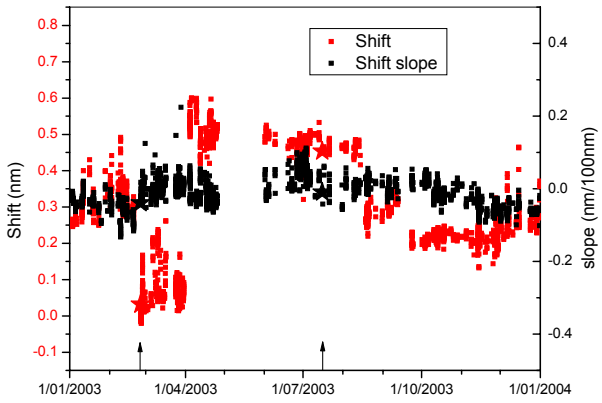

Figure 4. Calculated shift for the spectra recorded in 2003. This is all data for which a sunphotometer comparison was possible (implying that the sun was visible for the time period of the measurement). The two points marked by arrows indicate when manual Hg lamp calibrations were performed, and the results are marked by stars. At both times the wavelength scale was adjusted.

3.2. *Direct beam calculation*

The direct beam signal from the spectrometer needs to be calculated for all wavelengths from the alternating global and diffuse measurements via:

$$Direct_{\lambda} = (Global_{\lambda} - Diffuse_{\lambda})/\cos(sza) \qquad (1)$$

where *sza* is the solar zenith angle relevant to each measurement. In practice the direct beam irradiance for scan *i* is estimated by:

$$Direct_{\lambda,i} = \left|S_{\lambda,i} - S'_{\lambda,i-1,i+1}\right|/\cos(sza) \qquad (2)$$

where S' is an interpolated estimate of the signal from the preceding and next scans. The interpolation is done using the air mass values for the measurements as the *x* values, and log(*S*) as the *y* values. No correction has been applied for the shading caused by the arm supporting the shading disk. Estimates of the error associated with ignoring shading have been made by shifting the arm in and out of the field of view of the diffuser, using both 298 nm and 310 nm during the broken cloud conditions normally experienced at this site. The reduction in the global irradiance was estimated to be around 1.0±0.5%, where the uncertainty spans the range of 4 separate determinations measured near midday during summer. The impact will be higher at these high solar elevations, and so the effect will be less during the rest of the year.

3.3. *Comparison to the calibrated sunphotometer at λ_{ref}*

The sunphotometer measures direct beam irradiance, and is calibrated by other methods [e.g. Forgan, 1994]. The calibrated sunphotometer measurement is ratioed to the direct beam signal from SRAD at the same wavelength (341.6 nm in this case) to determine the instrumental sensitivity at this reference wavelength. This can only be done under clear sun conditions, which means that for a particular scan to produce an acceptable comparison, the sun needs to be unobstructed for the period from the start of the previous scan to the end of the following scan.

The calculation of the direct beam irradiance, given by equation (1), assumes that SRAD has an ideal angular (cosine) response. If this is not so, the ratio of the measurements between SRAD and the sunphotometer will show a dependence on solar elevation (and possibly azimuth). This provides an *in situ* check on the cosine response of the diffuser, whenever there is a period of clear sun. The outcome of such a test is shown in Figure 5 for 2002. The derived cosine response can be seen to be in agreement with the data provided by the manufacturer.

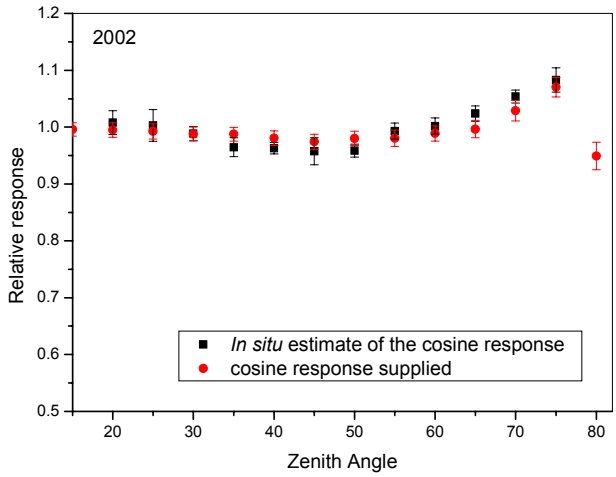

Figure 5. SRAD median sensitivity as a function of wavelength, derived from the ratio of SRAD to the sunphotometer for the period June - Dec 2002, compared with the cosine response supplied with the diffuser. The measurements have been binned into 5 degree increments. The error bars are 95% confidence intervals (black), and standard deviation (red).

The derived sensitivity of SRAD will vary with changing viewing conditions, even when using only unobstructed sun viewing conditions due to the changing nature of the diffuse irradiance. While this could be best eliminated through the use of only clear sky days, they are so rare at Cape Grim that this is not practicable. Therefore, it is necessary to average the estimates of the sensitivity. The calibrations generated by this process are shown in Figure 6. It can be seen that the calibrations remain stable over reasonably long periods of time, although the determination of the sensitivity from any particular day is relatively noisy. Also shown on the figure are the averages used to represent this data in the generation of the final calibrated data set. The final estimate in the uncertainty in the absolute calibration has been based on the assumption that the sensitivity at the reference wavelength has remained stable through the periods indicated in the figure. The absolute calibration (and its uncertainty) is then determined from the uncertainty in the calibration of the sunphotometer and in the determination of the mean value over the periods (which can be estimated to be 1% (95% confidence)). This assumption, however, may not be valid. The large temperature dependence of the spectrometer, and the critical dependence of the sensitivity to photomultiplier voltage, which is not independently assessable can both cause changes in sensitivity. If these sensitivities are changing on a daily basis an upper estimate of the uncertainty of around 8% (95% confidence limit) can be made, based on an analysis of the scatter in the retrieval from 2003. The values in Table 2 reflect the assumption of the noise being due to the variations during the estimate of the direct beam irradiance.

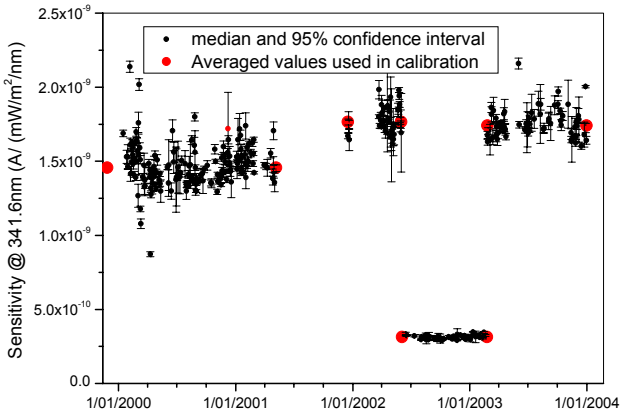

Figure 6. Calibration of direct beam sensitivity of SRAD via the SPO1-A sunphotometer channel at 341.6 nm. The period of low sensitivity in early 2003 was due to the SRAD controller reseting the system gain to a lower level following a power failure. The red stars mark the average calibration used for processing SRAD data.

Table 2. The 95% confidence intervals for the calibration of SRAD, excluding the uncertainty in the SUSIM reference spectrum based on the scatter in 2003 retrievals. R/L = ratio - Langley method. Midday = method outlined in the text. The relative sensitivity includes the uncertainties for the relevant combination of calibration methods listed, plus a reduction in uncertainty as a result of the smoothing of the final derived sensitivity. The abs. cal. sensitivity includes the scatter in the ratios of SRAD to the sunphotometer and the scatter in the calibration of the sunphotometer, estimated to be 1.5% based on the scatter in the calibrations.

Wavelength (nm)	R/L	midday	Rel. Sens.	Abs. Cal.	Total Uncertainty
300	9.9	1.06	2.3	2	3.0
305	5.5	0.50	2.3		3.0
315	2.6		1.4		2.4
340	0.4		0.2		2.0
395	1.0		0.6		2.1

3.4. Relative calibration at wavelengths other than λ_{ref}

On sunny mornings and afternoons SRAD can be calibrated relative to λ_{ref} through variations on the Langley method (an implementation of the Beer-Lambert-Bouguer law). That is, the following relationship will hold (at infinitesimally small wavelength resolution):

$$\ln\left(\frac{S_\lambda^0}{S_\lambda}\right) = \sum_i m_i \delta_{i\lambda} \qquad (3)$$

where *i* is a sum over Rayleigh (molecular) scattering, molecular absorption and aerosol scattering/ absorption (optical depth); m_i is the air mass relevant to the quantity *i* [Forgan, 1988a] and δ_i is the optical depth of that component. If the atmosphere is constant, a series of measurements made at differing air masses should then obey a simple linear relationship when $\ln(S_\lambda)$ is plotted as a function of *m*. The intercept at zero air mass is the 'calibration'. In principle such an approach could be used to determine S^0 at all wavelengths. However, varying sky condi-

tions make this unreliable under Cape Grim conditions, and so alternate strategies such the ratio-Langley method need to be used [Forgan, 1988b; Wilson and Forgan, 1995]. The ratio-Langley technique does not use the absolute signal, but the ratio of the signal at a wavelength to that of a reference wavelength. As has been shown by Forgan [1988b], the variations in the observed signal due to atmospheric conditions are often similar at various wavelengths, meaning that the ratio is more stable than the signals by themselves. This can be expressed via the equation:

$$\ln\left(\frac{S_{\lambda 2}}{S_{\lambda 1}}\right) = \ln\left(\frac{S^0_{\lambda 2}}{S^0_{\lambda 1}}\right) - \sum_i m_i \Delta\delta_i \qquad (4)$$

Here $\Delta\delta_i$ is the difference in optical depth between the two wavelengths. The advantage of the method lies in the fact that the difference in optical depth is more stable than the absolute value of the optical depth, especially for aerosol. Provided the $\Delta\delta_i$ are stable during the period used for the calibration determination, a valid estimate of the ratio of top of the atmosphere signals will be obtained.

This calibration is carried out during any period of the morning or afternoon where clear sun conditions occur over a suitable air mass range (for SRAD this is typically between an air mass of 1.8 and 3). However, for shorter wavelengths (less than 305 nm) the calibration has been found to be unstable. The total optical depth at these wavelengths is very large, due to both ozone absorption and Rayleigh scattering. This leads to a very restricted range of air masses at which there is a good signal to noise ratio. This is further exacerbated by the low ratio of direct to global irradiance, further reducing the direct beam signal-to-noise ratio.

To overcome the wavelength restrictions outlined above, a separate calibration is done over the middle of the day for wavelengths less than 305 nm. For this process it is assumed that the calibration for wavelengths greater than 305 nm is well known. The relation given in equation (4) is still used, although it is now used on individual spectra. It can be rewritten as:

$$\ln\left(\frac{S_{\lambda 2}}{S_{\lambda 1}}\right)(t) = \ln\left(\frac{S_{\lambda 2}}{S_{\lambda 1}}\right)(t) - m_{Rayleigh}\Delta\delta_{Rayleigh} - m_{O_3}\Delta\delta_{O_3} \qquad (5)$$

The reference wavelength used is 312.1 nm. The Rayleigh term is determined from measurements of air pressure and time [Bodhaine *et al*., 1999]. To determine the ozone impact, the ozone column is estimated from the direct beam irradiance estimates at wavelengths greater than 305 nm, using the ratios of measurements at set wavelength pairs in a manner equivalent to ozone determinations using a Dobson spectrometer [Komhyr *et al*., 1993]. In this case the ozone retrieval from wavelength pairs B (308.8/329.2 nm) and C (311.5/332.5 nm) are averaged. It is assumed that the aerosol optical depth component ($\Delta\delta_{aerosol}$) is zero, as this relationship is being used over such a small wavelength range (<15 nm). With this information each spectrum can be used to determine each term on the right hand side of equation (5), thereby giving an estimate of the relative calibration. This is carried out for all spectra collected between 11:30 and 14:00 when the sun is visible, and the values for the day averaged.

An example of the output of this process is shown in Figure 7. As this is an estimate of the ratio of the instrumental signal at the top of the atmosphere, the fine structure observed is due to the structure in the solar spectrum. This can be seen by comparison with the SUSIM spectrum which is included in the plot. The ratio retrieved by the two methods are very similar, both in magnitude and uncertainty, above 305 nm. Below 305 nm the midday method gives a smaller scatter, as can be seen from the uncertainty estimates in Table 1. For the final processing the two wavelength-based calibrations are joined at 312 nm.

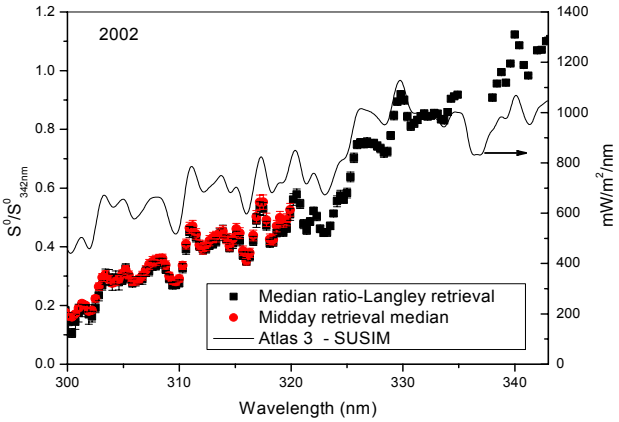

Figure 7. The calibration relative to 341.6 nm for the year 2002. The black points are the median values determined using the ratio-Langley technique on 90 half days during the year. The red are those retrieved using 17 midday measurement sets, as outlined in the text. The error bars are one standard error, in both cases. For the midday retrievals, the error estimate includes the uncertainty in the reference value at 312.1 nm. The continuous line is the top of the atmosphere spectrum recorded on Atlas 3 with SUSIM [van Hoosier *et al*., personal communication, 1996].

These methods determine the signal for the instrument at the top of the atmosphere, relative to the signal at the reference wavelength. To determine the actual instrument wavelength sensitivity, it is necessary to know the irradiance at the top of the atmosphere. Once again, the SUSIM solar spectrum is used [see equations 7 and 8 in Wilson and Forgan, 1995]. The wavelength dependence of the sensitivity of the instrument changes slowly, so the relative calibrations normally agree within their uncertainty over periods up to years. The averages of the calibrations are shown in Figure 8, along with the standard deviations for the sensitivity calculated for each wavelength separately. This standard deviation will

include variation due to residual wavelength errors and the noise in the original measurements. As the wavelength calibration should be a relatively smooth function of wavelength, a 1.5 nm wide, low-pass Fourier transform filter has been used to determine the final wavelength calibration and this is shown in the figure. Given the number of points involved, this reduces the scatter in the results by approximately a factor of 2. The upper panel of Figure 8 shows that while the deviations between the individual points may exceed 5%, with this small (and realistic) level of smoothing the two calibrations agree to within 2% at all wavelengths except at the end of the measured range which are perturbed by the wavelength correction process. This is within the 95% uncertainty estimates for the calibrations (Table 2), confirming the stability of the wavelength sensitivity.

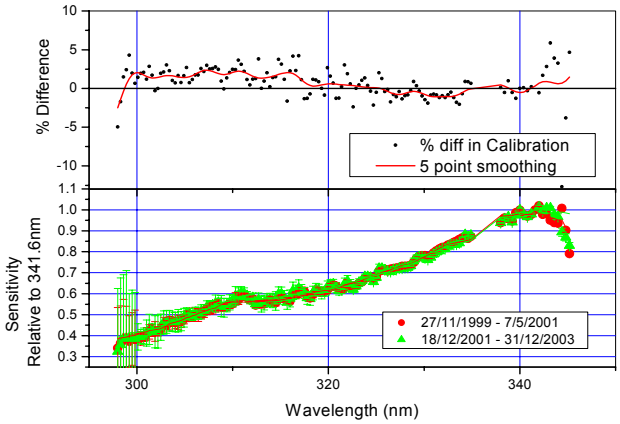

Figure 8. The wavelength calibration for SRAD, relative to the sensitivity at 341.6 nm. The individual points represent the values derived for each wavelength, independent of the neighbouring wavelengths. The solid red line represents a 1.5 nm smoothing of the data, which is used to define the calibration. The bottom panel shows the calibration derived for the two periods, the upper panel shows the differences between the two calibrations.

The output from the steps outlined above defines the calibration of the instrument. All spectra are then processed to produce estimates of spectral irradiance as a function of wavelength. In addition, estimates of the integrated irradiance are determined, both for the UV-B region (both diffuse and global), and the erythemal irradiance [McKinlay and Diffey, 1987]. The estimates of the integrated quantities do not include any correction for the missing UV-B component below 298 nm, as the correction is very small. These data reside in the Cape Grim database for at least the period 2000 – 2003.

4. Comments and conclusions

The spectrometer SRAD has been operating for a number of years, and is now producing calibrated data. Table 2 lists the 95% confidence intervals estimated for the instrument based on the scatter in the calibrations for 2003. This is typical of what is observed for all the other years, except for 2002, where the scatter is a factor of two larger. This is presumably due to the very low sensitivity for much of the year (see Figure 6). Note that the error estimates presented include no error in the SUSIM spectrum. While this is appropriate if other instruments use the same spectrum as their final calibration standard, for those systems using standard lamps the error budget must be expanded to include the SUSIM uncertainty. This is estimated to be of the order of 3.5% [Thuillier *et al*., 2004].

The instrumentation has some limitations. First, the passive nature of the sun tracking means that the diffuse measurement may be in error and there is no direct measure of the problem. However, such errors, when due to slipping tracker drives, will be detected through the tracker zeros. As noted, there is no significant change in the retrieved calibration when zero error filters have been added to reject data potentially affected by this problem.

Secondly, the instrumental calibration depends on the determination of the direct beam irradiance, which is not directly measured. This introduces a need for constant viewing conditions for both the determination of the absolute calibration at the reference wavelength and in the relative calibration for the period of at least twice the time of the spectral scan. In the current configuration, this is a period of over 10 minutes. This introduces much of the scatter evident in the calibrations (e.g. Figure 6). It may be possible to assess the impact of this by using a data filter based on broad band measurements, in either visible or UV-B regions. This will need to be investigated in the future. The effect should be random, however, and so should not introduce a bias in the calibration, permitting the accuracy of the central estimate to be improved by the use of the multiple calibrations.

Thirdly, the temperature sensitivity of the spectrometer is quite large, and quite small changes in temperature may induce large variations in sensitivity. Tests on this effect have only been carried out using diffusers with relative large cosine errors, which can mask the retrieval of the temperature dependence. Clearly the temperature dependence could be the limiting factor to the accuracy of individual measurements, and unfortunately the temperature is only available indirectly from the wavelength shift. It would be useful to re-examine the temperature dependence using the NIWA diffuser described here.

Finally, the spectrometer and controller is a reasonably complex instrument, and has been prone to failure, as has been documented in previous editions of *Baseline*. This has led to significant gaps in the data record.

A replacement system is currently being developed, which addresses some of these limitations. In particular, the instrument will measure direct beam and diffuse irradiance, rather than global and diffuse, which should make the retrieval much more robust. Secondly, the spectrometers do not scan, but use array detectors. This should permit much more reliable operation under the maritime conditions experienced at Cape Grim.

References

Andrady, A. L., H. S. Hamid, and A. Torikai, Effects of climate change and UV-B on materials, *Photochem. and Photobiol. Sci.*, *2* (1), 68-72, 2003.

Atkinson, R., D. L. Baulch, R. A. Cox, J. N. Crowley, R. F. Hampson, R. G. Hynes, M. E. Jenkin, M. J. Rossi, and J. Troe, Evaluated kinetic and photochemical data for atmospheric chemistry: Volume I - gas phase reactions of O_x, HO_x, NO_x and SO_x species, *Atmos. Chem. and Phys.*, 4, 1461-1738, 2004.

Bodhaine, B. A., N. B. Wood, E. G. Dutton, and J. R. Slusser, On Rayleigh optical depth calculations, *J. Atmos. and Oceanic Tech.*, 16 (11 Part 2), 1854-1861, 1999.

Caldwell, M. M., C. L. Ballaré, J. F. Bornman, S. D. Flint, L. F. Björn, A. H. Teramura, G. Kulandaivelu, and M. Tevini, Terrestrial ecosystems, increased solar ultraviolet radiation and interactions with other climatic change factors, *Photochem. and Photobiol. Sci.*, *2*, 29-38, 2003.

Chipperfield, M. P., W. J. L. A. Randel, G. E. Bodeker, M. Dameris, V. E. Fioletov, R. R. Friedl, N. R. P. Harris, J. A. Logan, R. D. McPeters, N. J. Muthama, T. Peter, T. G. Shepherd, K. P. Shine, S. Solomon, L. W. Thomason, and J. M. Zawodny, Global Ozone, Past and Future, Chapter 4, in *Scientific Assessment of Ozone Depletion: 2002, Global Ozone Research and Monitoring Project-Report No. 47*, World Meteorological Organization, Geneva, 2003.

Creasey, D. J., G. E. Evans, D. E. Heard, and J. D. Lee, Measurements of OH and HO_2 concentrations in the Southern Ocean marine boundary layer, *J. Geophys. Res.*, 108(D15), 4475, 2003.

de Gruijl, F. R., J. Longstreth, M. Norval, A. P. Cullen, H. Slaper, M. L. Kripke, Y. Takizawa, and J.C . van der Leun, Health effects from stratospheric ozone depletion and interactions with climate change (vol 2, pg 16, 2003), *Photochem. and Photobiol. Sci.*, 2(3), 354-354, 2003.

Forgan, B. W., Bias in a solar constant determination by the Langley method due to structured atmospheric aerosol: comment, *Appl. Opt.*, *27* (12), 2546-2548, 1988a.

Forgan, B. W., Sunphotometer calibration by the ratio-Langley method, in *Baseline Atmospheric Program (Australia) 1986*, edited by B. W. Forgan, and P. J. Fraser, Bureau of Meteorology and CSIRO Division of Atmospheric Research, Melbourne, Australia, 22-26,1988b.

Forgan, B. W., General method for calibrating sun photometers, *Appl. Opt.*, *33* (21), 4841-4850, 1994.

Hader, D. P., H. D. Kumar, R. C. Smith, and R. C. Worrest, Aquatic ecosystems: effects of solar ultraviolet radiation and interactions with other climatic change factors, *Photochem. and Photobiol. Sci.*, 2(1), 39-50, 2003.

Kerr, J. B., G. L. A. Seckmeyer, A. F. Bais, G. Bernhard, M. Blumthaler, S. B. Diaz, N. Krotkov, D. Lubin, R. L. McKenzie, A. A. Sabziparvar, and J. Verdebout, Surface ultraviolet radiation: Past and future, Chapter 5, in *Scientific Assessment of Ozone Depletion: 2002, Global Ozone Research and Monitoring Project-Report No. 47*, World Meteorological Organization, Geneva, 2003.

Komhyr, W. D., C. L. Mateer, and R. D. Hudson, Effective Bass-Paur 1985 ozone absorption coefficients for use with dobson ozone spectrophotometers, *J. Geophys. Res.*, 98(D11), 20451-20465, 1993.

McKenzie, R. L., L. O. Bjorn, A. Bais, and M. Ilyas, Changes in biologically active ultraviolet radiation reaching the Earth's surface, *Photochemical and Photobiol. Sci.*, *2* (1), 5-15, 2003.

McKinlay, A. F., and A. F. Diffey, A reference action spectrum for ultraviolet induced erythema in human skin, in *Human Exposure to Ultraviolet Radiation. Risks and Regulations*, edited by W. F. Passchier and B. F. M. Bosnjakovic, Elsevier Science, Amsterdam, 83-87, 1987.

Pye, S. D., and C. J. Martin, A study of the directional response of ultraviolet radiometers: I. Practical evaluation and implications for ultraviolet measurement standards, *Physics in Medicine and Biology*, *45* (9), 2701-2712, 2000.

Sander, S. P., B. J. Finlayson-Pitts, R. R. Friedl, D. M. Golden, R. E. Huie, C. E. Kolb, M. J. Kurylo, M. J. Molina, G. K. Moortgat, V. L. Orkin, and A. R. Ravishankara, Chemical kinetics and photochemical data for use in atmospheric studies, Evaluation number 14, Jet Propulsion Laboratory, Pasadena, 2002.

Slaper, H., H. Reinen, M. Blumthaler, M. Huber, and F. Kuik, Comparing ground-level spectrally resolved solar UV measurements using various instruments - a technique resolving effects of wavelength shift and slit width, *Geophys. Res. Letts.*., *22* (20), 2721-2724, 1995.

Thuillier, G., L. Floyd, T. N. Woods, R. Cebula, E. Hilsenrath, M. Herse, and D. Labs, Solar irradiance reference spectra for two solar active levels, *Adv. in Space Res.*, *34*, 256-261, 2004.

Wilson, S. R., and B. W. Forgan, *In situ* calibration technique for UV spectral radiometers, *Appl. Opt.*, *34* (24), 5475-5484, 1995.

Zepp, R. G., T. V. Callaghan, and D. J. Erickson, Interactive effects of ozone depletion and climate change on biogeochemical cycles, *Photochem. and Photobiol. Sci.*, *2* (1), 51-61, 2003